Lithos xxx (2009) xxx–xxx

Contents lists available at ScienceDirect

Lithos

journal homepage: www.elsevier.com/locate/lithos

Metasomatic origin of diamonds in the world's largest diamondiferous eclogite

Yang Liu [a,*], Lawrence A. Taylor [a], Amit Basu Sarbadhikari [a], John W. Valley [b], Takayuki Ushikubo [b], Michael J. Spicuzza [b], Noriko Kita [b], Richard Ketchum [c], William Carlson [c], Vladislav Shatsky [d], Nikolai V. Sobolev [d]

[a] Planetary Geosciences Institute, Dept. of Earth and Planetary Sciences, The University of Tennessee, Knoxville, TN 37996, USA
[b] WiscSIMS, Dept. of Geoscience, University of Wisconsin, 1215 W Dayton St. Madison WI 53706, USA
[c] Dept. of Geological Sci., Univ. of Texas, Austin, TX 78712, USA
[d] V.S. Sobolev Institute of Geology and Mineralogy, Russian Academy of Science-Siberian Branch, Novosibirsk 630090, Russia

ARTICLE INFO

Article history:
Received 29 September 2008
Accepted 5 June 2009
Available online xxxx

Keywords:
Eclogite xenolith
Diamond
Metasomatic origin
Carbon isotopes
SIMS

ABSTRACT

The world's largest diamondiferous eclogite (8.8 kg, UD-111/02) from the Udachnaya kimberlite, Siberia, is the subject of this investigation. High-resolution X-ray computed tomography (HRXCT), chemistry of host minerals and diamond inclusions, stratigraphy of the diamonds (cathodoluminescence zoning), and carbon isotopes have been obtained. HRXCT images, 3-d models, and subsequent detailed dissection of this Group B eclogite revealed linear distributions of diamonds along alteration zones. Both unusual multiple-diamond clusters with dodecahedral morphologies, and distinctive internal zoning recorded by cathodoluminescence analyses are indicative of multiple stages of diamond growth and resorption in UD-111-02. Carbon-isotope ratios ($\delta^{13}C$) of 16 diamonds have a total range of ~7‰ (−2.0 to −9.2‰), with the majority at −5.4‰. Diamond core values are variable and include the lightest (−9.2‰) and heaviest $\delta^{13}C$ (−2.0‰) values, suggesting that cores formed from distinct carbon sources, or grew under different conditions. In contrast, the rims of all diamonds have similar $\delta^{13}C$ values (average −5.2‰ with a 2SD of 1.2‰), suggesting that they formed under uniform conditions. Mineral inclusions in diamonds display compositional variations. These lines of evidence, considered together, indicate that diamonds in this eclogite were formed by several events, most likely from multiple metasomatic fluids. Furthermore, it is becoming increasingly evident that in most diamondiferous eclogites, diamonds are not synchronously formed with their host eclogites.

1. Introduction

Diamondiferous eclogite xenoliths are rare mantle samples delivered to the Earth's surface by kimberlites. Most of diamondiferous eclogites are of Archean age, and thus, contain important information on early crustal and mantle processes (Pearson et al., 2003). It is generally agreed that diamondiferous eclogites are of crustal origin; they are basically metamorphosed restites after partial melting of subducted oceanic crust (Jacob, 2004; Taylor and Anand, 2004; Jacob et al., this issue). Also known is the fact that many diamonds have crustal signatures based upon: 1) oxygen isotopes in the eclogites and their diamond mineral inclusions (Snyder et al., 1995; Lowry et al., 1999; Schulze et al., 2003; Anand et al., 2004; Spetsius et al., 2008); 2) carbon of probable crustal source, with large negative $\delta^{13}C$ values (−20 to −41‰) of the diamonds (Kirkley et al., 1991; Cartigny, 2005; De Stefano et al., 2008; Spetsius et al., this issue); 3) a wide range of sulfur isotopes ($\delta^{34}S$) in sulfide inclusions (Chaussidon et al., 1987; Eldridge et al., 1991; Deines and Harris, 1995; Ruzicka et al., 1999); and 4) the presence of positive and negative Eu anomalies in some diamond inclusions (Jerde et al., 1993; Taylor et al., 2000; Stachel and Harris, 2008).

Diamonds in eclogites are generally considered to grow from metasomatic carbonate-rich fluids in the mantle, based upon extensive high-pressure experimentation, and supported by the presence of carbonate and CO_2-rich fluid inclusions, particularly in the outer portions of many diamonds (references in Taylor and Anand, 2004). Indeed, the natural setting of diamonds in their eclogite host rocks, as well as the mineral inclusions in the diamonds recovered from such xenoliths provides additional support for the metasomatic origin (Taylor and Anand, 2004; Stachel and Harris, 2008). In addition, there is a wide range of compositions of inclusions among diamonds within the same xenolith, suggesting multi-stage growth of diamonds (e.g., Taylor and Anand, 2004). Recently, the recovery of a large diamondiferous eclogite (8.8 kg, UD-111/02) from the Udachnaya kimberlite, Russia (Taylor et al., 2005; Stepanov et al., 2007, 2008), exceeded a previous find of an 8.6 kg eclogite from the Roberts Victor kimberlite in South Africa (Jacob and Jagoutz, 1994). Our results on this new eclogite, along with those from Stepanov et al. (2007, 2008), also suggest multiple-stage formation of diamonds in this eclogite. In addition, we report the first discovery of clusters of several intergrown diamonds exhibiting *dodecahedral* morphologies in an eclogite.

* Corresponding author. Tel.: +1 865 974 6024; fax: +1 865 974 2368.
E-mail address: yangl@utk.edu (Y. Liu).

0024-4937/$ – see front matter © 2009 Published by Elsevier B.V.
doi:10.1016/j.lithos.2009.06.036

Combined with findings on other smaller diamondiferous eclogites (Keller et al., 1999; Taylor et al., 2000; Anand et al., 2004; Ishikawa et al., 2008; Taylor, unpublished data), we argue that diamonds in many diamondiferous eclogites have experienced multiple metasomatic events during their growth and are formed non-synchronously from their host eclogites.

2. Methods

2.1. Tomography

High-resolution X-ray computed tomography (HRXCT) provides a non-destructive, *in-situ* method to study the internal textures of rocks (Carlson and Denison 1992, Rowe et al., 1997). The method used for this study was similar to those described in Taylor et al. (2000) and Anand et al. (2004). Due to size limitations for the HRXCT scanning, a relatively small mass of the entire 8.8 kg xenolith was broken off. The mass of this specimen (0.5 kg, ~10×7×4.5 cm), coupled with the respective densities of the minerals, posed challenges (artifacts and low resolution) for HRXCT using the routine settings (100 kV). Instead, two X-ray energies (100 kV and 180 kV) were used to enhance mineral recognition differentially. A series of 450, 2-D X-ray slices was obtained on this eclogite at each voltage, using a micro-focal X-ray source and an image-intensifier detector system to measure the absorption of X-rays along numerous coplanar paths through the sample. The slice thickness was 159 μm, and the distance between each slice is ~100 μm. The two complete sets of slices at the two voltages were superimposed to get the best color contrast between the minerals (Fig. 1). The in-plane resolution is ~50 μm. These 2-D images were stacked together using volume-visualization software to produce a 3-D model of the xenolith. Minerals were differentiated based on their different X-ray attenuation values, increasing from sulfides (white Fig. 1), to garnets, to clinopyroxene, to secondary minerals, and to diamonds (black, Fig. 1). In one 3-D model, the silicates were made transparent in order to display only the diamonds and sulfides. Relationships between mineral phases were determined by rotating and viewing the 3-D model at different perspectives to look for any mineral associations, alignments, or fabrics.

2.2. Dissection and sample preparation

Based upon the HRXCT mapping, a detailed dissection (pull-apart) of the xenolith was conducted in order to recover the diamonds, as well as to examine their relationships to the host minerals. The nature and physical properties of minerals in direct contact with the diamonds were carefully examined. Diamonds extracted from different locations inside the rock were selected for further study. Twenty four diamonds were cut near {110} to obtain a large cross-sectional area with near-vertical zonation contacts, as seen with cathodoluminescence. Some of these diamonds were cut to simultaneously expose 2–3 inclusions. Cut diamonds were then cleaned with distilled water and mounted in epoxy, using a routine developed at the University of Wisconsin, so as to insure all diamond polished surfaces were at the same z-position in the mount.

Cathodoluminescent (CL) imaging was used to reveal the internal growth zones ('stratigraphy'; oscillatory zones) of the diamonds and the

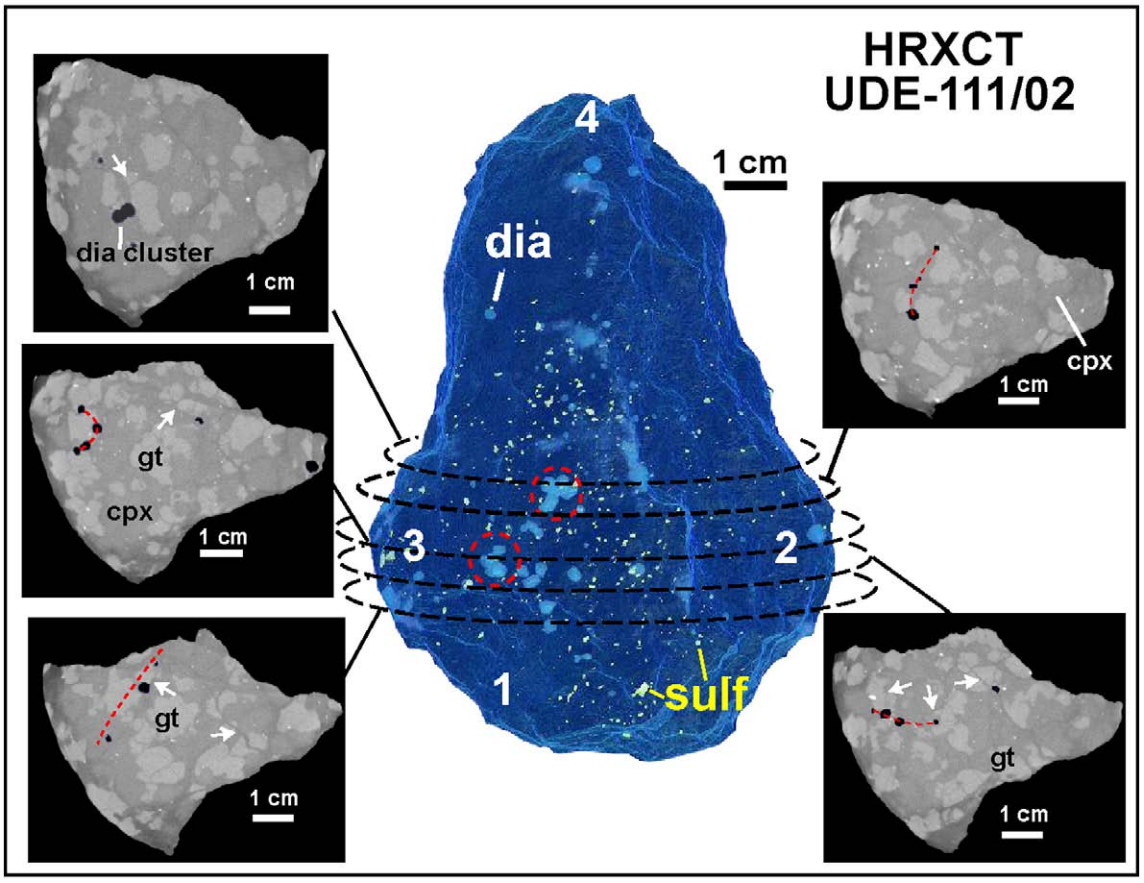

Fig. 1. Tomography of diamondiferous eclogite UD-111/02 from Udachnaya. Center: a 3-d model of UD-111/02 based on HRXCT. Light blue grains are diamonds, and yellow specs are sulfide minerals. Garnet and clinopyroxene crystals were rendered invisible to improve the clarity. Red circles outline the diamond clusters found with dodecahedral morphology (Fig. 2c-d). Numbers 1–4 mark locations of pristine host minerals analyzed by electron microprobe. Figures on left and right of the central image are 2-D X-ray slices obtained originally by the HRXCT technique from the level outlined by the dashed girdle around the eclogite. In these slices, diamond appears black, garnet as light gray, clinopyroxene as dark gray, and sulfide as white. Lineations of multiple diamonds appear in two slices on the lower left and two on the right. White arrows mark the alteration veins.

Please cite this article as: Liu, Y., et al., Metasomatic origin of diamonds in the world's largest diamondiferous eclogite, Lithos (2009), doi:10.1016/j.lithos.2009.06.036

abnormal variations (rounded corners, healed fractures, jagged cores). These CL images were collected using a cold-cathode CL microscope at the University of Tennessee. For the CL microscope, an electron beam voltage of ~5 kV and 0.25 mA was used to generate the luminescence on the diamond polished surfaces without any carbon coating. Color CL images of eight diamonds were collected. However, to minimize beam damage to the epoxy, grayscale CL images, which require shorter exposure times, were collected for the rest of diamonds.

2.3. Carbon-isotope ratios

In-situ carbon-isotope analyses of different CL zones in the cut diamonds were obtained using the CAMECA IMS-1280 at the University of Wisconsin (Kita et al., 2009). The diamond mounts were coated with a thin Au film. A $^{133}Cs^{+}$ primary ion beam (20 kV total acceleration voltage) was set at 0.7 nA (~7 μm in diameter). Secondary ions were extracted with a 10 kV voltage and selected using a 40 eV energy window. Mass-resolving power was set to ~3000, which is enough to eliminate the $^{12}CH^{-}$ interference to $^{13}C^{-}$. The sample was pre-sputtered for 70 s to remove the Au coating and automatic centering of secondary ions. Two carbon isotopes ($^{12}C^{-}$ and $^{13}C^{-}$) were measured for 80 s simultaneously with two Faraday cups. Analyses on UD-111/02 diamonds were bracketed with 8 to 12 analyses on an in-house standard (a Kelsey Lake diamond, KLD-9.41) to correct for instrumental bias. The $\delta^{13}C$ of KLD-9.41 (-5.9‰ PDB with a 2 standard deviation, 2SD, of ± 0.2 for $n=4$) was measured by combustion to CO_2 and gas-source mass spectrometer also at the University of Wisconsin-Madison. Values of $\delta^{13}C$ are reported in standard per mil notation and normalized to the PDB standard. The spot-to-spot reproducibility of $\delta^{13}C$ was typically 0.5‰ (2SD).

2.4. Mineral chemistry

Compositions of the host garnet, clinopyroxene, and sulfide minerals, as well as the mineral inclusions in diamond, were analyzed using a Cameca SX50 electron microprobe at the University of Tennessee. Analytical conditions for host silicates included an accelerating voltage of 15 kV, a beam current of 20 nA and a beam size of 1–5 μm. The large beam size (5 μm) was used for clinopyroxene, to minimize loss of Na during the analysis. Analytical conditions for sulfides were an accelerating voltage of 15 kV, a beam current of 10 nA, and a beam size of 10 μm. Counting time for all elements was 20 s, except for K in clinopyroxene (40 s), and Co, Ni, and Cu in sulfides (40, 40, and 30 s, respectively). The Au coats on epoxy discs were removed by gentle polishing and the epoxy discs were re-coated with carbon. Analytical conditions for mineral inclusions in the diamonds included an acceleration voltage of 20 kV, a beam current of 10 nA, and a beam size of 2 μm. Na, Cr, and Mn in mineral inclusions were counted longer (30 s). The standard Cameca PAP corrections were applied to the resulting dataset.

3. Results

3.1. Internal texture of diamondiferous eclogites

In spite of the difficulties caused by the large sample size (Section 2.1), HRXCT imaging successfully revealed >100 macro-diamonds (1–5 mm) and two clusters of diamonds (Fig. 1). Sulfide minerals appear to be randomly distributed throughout the sample, with no apparent association with the diamonds (Fig. 1). Micro-diamonds (<1 mm), undetected in the HRXCT, are often present in close proximity to larger diamonds. No diamonds either visible in HRXCT imaging or revealed during the subsequent xenolith dissection were located within primary minerals (Fig. 2). These diamonds are always interstitial to the primary host garnet and omphacite (inside alteration veins). Indeed, several diamonds form lineations (some resembling chains) along structurally weak zones, which appear to have had increased permeability for fluid migration (e.g., alteration veins) throughout the sample (Figs. 1 and 2).

Two small diamond clusters (5–10 mm long) were recovered from near the center of this large eclogite in association with entirely fresh

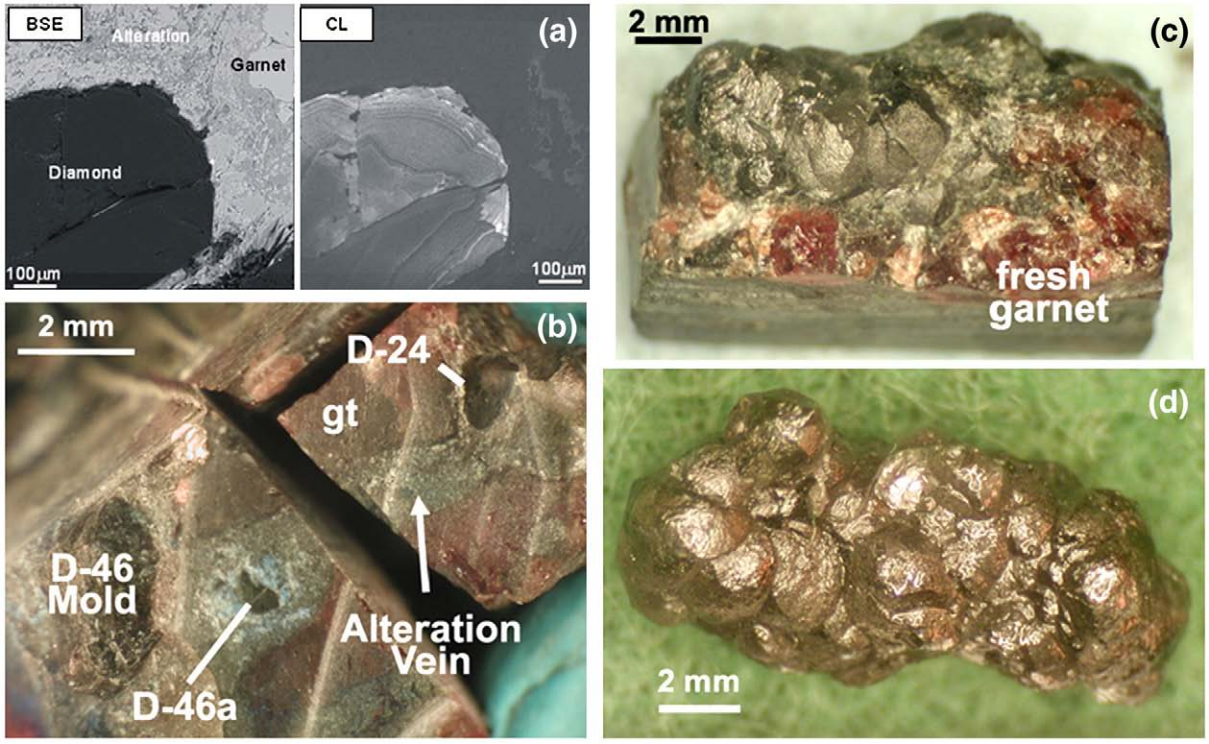

Fig. 2. Natural setting of diamond in UD-111/02. (a) BSE and cathodoluminescence (CL) images of a small diamond in a polished section of UD-111/02. (b) Alignment of several diamonds in an alteration vein observed during the eclogite dissection. (c) Resorbed and coated multi-crystalline diamond aggregates before extraction. (d) The same diamond cluster in (c) after dissolving silicates in HF. Individual diamonds display round edge and dodecahedral morphology indicative of resorption (McCallum et al., 1994).

Please cite this article as: Liu, Y., et al., Metasomatic origin of diamonds in the world's largest diamondiferous eclogite, Lithos (2009), doi:10.1016/j.lithos.2009.06.036

garnet, albeit not in direct contact. One cluster is shown in Fig. 2c–d. The diamonds in these clusters have been extensively resorbed, displaying round edges and dodecahedral morphology. Diamonds of dodecahedral shape are rare in eclogites, but individual dodecahedral stones were identified in diamondiferous eclogites from South Africa (Robinson, 1979).

3.2. Petrography and host mineralogy of UD-111/02

Based on the tomography, UD-111/02 consists mainly of ~65 vol.% clinopyroxene and 35 vol.% garnet (Fig. 3a), which is within the reported modal range for Udachnaya eclogites (e.g., Sobolev et al., 1994; Taylor et al., 2000). Individual pristine grains of host minerals from various locations in the xenolith have different compositions (e.g., 4.7 to 6.6 wt.% Na_2O for clinopyroxene, Table 1, Fig. 4), possibly reflecting a heterogeneous protolith. Clinopyroxenes in the host eclogite are typically omphacitic. According to the classification by Taylor and Neal (1989), UD-111/02 clinopyroxenes plot in the field of Group B eclogites in a MgO–Na_2O plot (Fig. 4e). The clinopyroxenes have moderate Na_2O and MgO contents compared to other eclogitic xenoliths from the Udachnaya pipe. The omphacite commonly contains the previously reported 'spongy texture' (Fig. 3b) of secondary pyroxenes in optical continuity with the primary pyroxene (Taylor and Neal, 1989; Sobolev et al., 1998a, 1999; Spetsius and Taylor, 2002; Misra et al., 2004). These secondary pyroxenes, compared to the original omphacites, have lower Na_2O and Al_2O_3, higher CaO and MgO contents. Clinopyroxenes associated with the spongy texture often possess a large range of compositions, consistent with metasomatically-induced, partial-melting event(s) (Spetsius and Taylor, 2002; Misra et al., 2004).

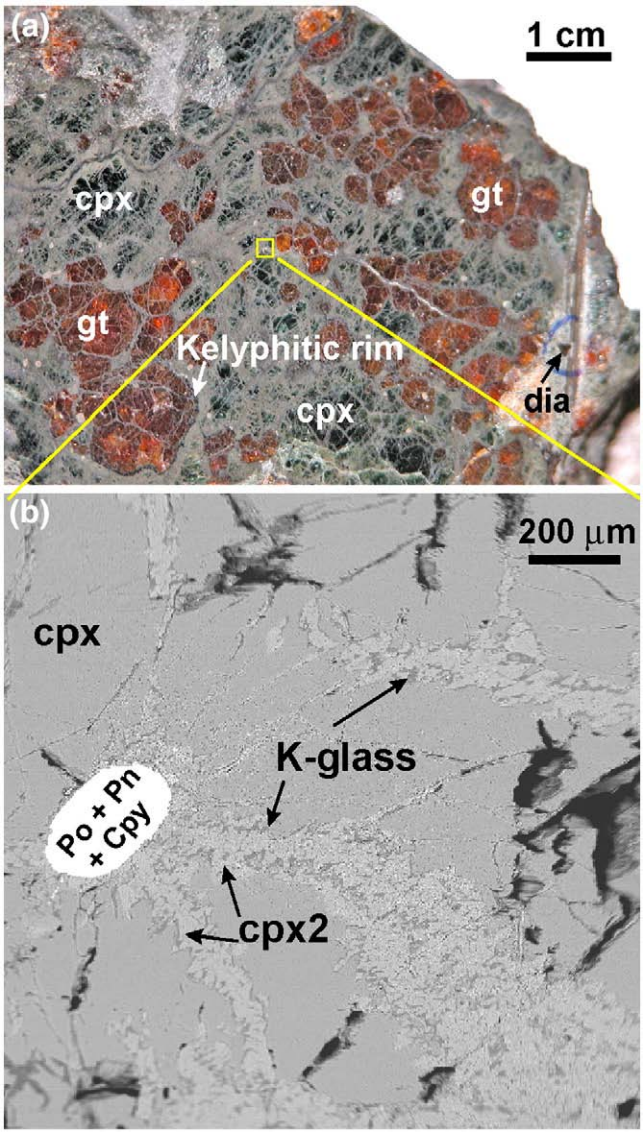

Fig. 3. Secondary alteration of host minerals in UD-111/02. (a) Kelyphitic rim around garnet grains; note the diamond to the right. (b) Spongy texture in the clinopyroxene due to the metasomatically-induced partial melting of the pyroxene, as detailed by Spetsius and Taylor (2002). Cpx2 is the secondary pyroxene with less Na_2O and Al_2O_3, and higher CaO. The fine-grain secondary products in the matrix include K–Na-rich glass and spinel.

Red-orange garnets occur as agglomerations of grains up to 1 cm in diameter with thin kelyphitic rims ~0.3 mm thick (Fig. 3a). Garnet compositions from different locations in the xenolith vary (Mg#: 60–70). The compositions of UD-111/02 garnet, in our 0.5 kg portion of this huge xenolith, range from 64% pyrope and 28% almandine to 54% pyrope and 34% almandine (Fig. 4b). The highest Mg# of host garnet (75) in UD-111/02 was reported by Stepanov et al. (2007). In comparison to other eclogitic xenoliths from the same pipe (e.g., Snyder et al., 1997; Sobolev et al., 1998a), UD-111/02 garnets contain higher MgO and Na_2O, but lie in the low-Ca end of the field (Fig. 4a, b). Using the classification of Taylor and Neal (1989), UD-111/02 garnet plots at the boundary between Group A and B eclogites (Fig. 4b).

These primary mineral compositions (Fig. 4) indicate that UD-111/02 is a Group B eclogite, similar to results of Stepanov et al. (2007, 2008). This type of eclogite is typical for diamondiferous eclogitic xenoliths from the Udachnaya kimberlite pipe (Sobolev et al., 1994; Sobolev et al., 1998a). Each garnet and clinopyroxene grain are homogeneous, and thus, they are considered to be in equilibrium. Owing to the heterogeneity among different grains from various parts of UD-111/02, adjacent garnet and clinopyroxene pair compositions (Table 1) were used for the estimates of temperature. The Fe–Mg exchange garnet–clinopyroxene geothermometer of Ellis and Green (1979) was used to estimate temperature as a function of pressure. Rather than assume a pressure, the geotherm of 40 mW/m^2 from Boyd et al. (1997) and Griffin et al. (1996) for Siberian craton was used to calculate the *P–T* curve. The intersection of these two *T–P* lines so utilized defines the pressure and temperature of that mineral assemblage. For garnet and pyroxene in UD-111/02, the two *T–P* lines intersect at 6.5 GPa with temperature of: a) ~1275 °C for garnet ($Py_{64}Al_{28}Gr_8$, molar Fe/Mg = 0.44) and pyroxene ($En_{52}Fs_{11}Wo_{37}$, Fe/Mg = 0.22), b) ~1255 °C for garnet ($Py_{56}Al_{35}Gr_9$, Fe/Mg = 0.62) and pyroxene ($En_{49}Fs_{14}Wo_{37}$, Fe/Mg = 0.26). These estimates are virtually identical to the values of 1260–1275 °C at 6.5 GPa for other diamondiferous eclogites from Udachnaya (U-51, U33/1, UX1; Taylor et al., 2000; Misra et al., 2004).

Sulfide minerals display major intergrowths of pyrrhotite ($Fe_{0.90-0.96}S$) and pentlandite, with lesser amounts of chalcopyrite (Table 1), a typical assemblage formed by subsolidus exsolution of a monosulfide solid solution (Mss) (see review by Taylor and Liu, 2009). Pentlandite mainly occurs as "widmanstätten-like" exsolution lamellae in pyrrhotite and also as flames on the rims of sulfide grains. Chalcopyrite typically occurs as a thin rim surrounding the pyrrhotite and pentlandite, but sometime occurs as flames or coarsened cells. These different textures as reviewed in Taylor and Liu (2009) reflect different cooling rates and degrees of saturation of the Mss as it cooled and exsolved the pyrrhotite + pentlandite + chalcopyrite, on the basis of kinetic experiments by Durazzo and Taylor (1982), Kelly and Vaughan (1983), and Etschmann et al. (2004).

3.3. UD-111/02 diamonds and their internal morphology

Most of the extracted diamonds are colorless, but a few are brown or pink. Most diamonds are octahedral or intergrown octahedra (combined form of Stepanov et al., 2007). Cubo-octahedral diamonds are found only as ≤1 mm crystals and in general, are distinctly closer to the small amount of kimberlite attached to one part of the xenolith.

Please cite this article as: Liu, Y., et al., Metasomatic origin of diamonds in the world's largest diamondiferous eclogite, Lithos (2009), doi:10.1016/j.lithos.2009.06.036

Table 1
Representative major-element compositions of pristine host minerals in eclogite xenolith UD-111/02[a].

Location	Cpx-a[a] 1	Cpx-b[a] 1	Cpx 2	Cpx 3	Cpx 4	Gt-a[a] 1	Gt-b[a] 1	Gt 2	Gt 3	Gt 4		Po	Pn	Cpy
SiO_2	55.5	55.6	55.7	55.3	55.9	40.4	41.3	40.7	41.4	40.1	S	38.4	32.7	37.5
TiO_2	0.51	0.57	0.50	0.56	0.56	0.45	0.49	0.42	0.48	0.47	Fe	61.4	30.0	29.5
Al_2O_3	9.52	7.79	10.2	7.76	8.09	22.4	22.7	22.3	22.7	22.1	Co	<0.03	1.80	<0.03
Cr_2O_3	0.05	0.05	<0.05	0.05	0.09	<0.05	<0.05	0.07	0.05	0.08	Ni	0.39	35.2	<0.03
MgO	10.7	12.6	10.2	12.7	11.6	15.3	17.8	15.3	18.0	16.1	Cu	0.06	<0.03	33.5
CaO	11.4	12.5	11.1	12.5	12.2	4.13	3.43	4.10	3.46	3.84	Si	<0.03	<0.03	0.23
MnO	0.08	0.07	0.10	0.10	0.06	0.33	0.31	0.31	0.28	0.31	total	100.3	99.6	100.8
FeO	5.53	5.00	5.23	5.06	5.66	17.0	13.9	16.5	14.0	16.0				
Na_2O	6.00	4.80	6.35	4.85	5.01	0.17	0.16	0.14	0.17	0.16				
K_2O	0.14	0.13	0.13	0.14	0.14	n.a.	n.a.	n.a.	n.a.	n.a.				
Totals	99.4	99.1	99.5	99.1	99.3	100.2	100.1	99.9	100.6	99.2				
Oxygen	6	6	6	6	6	12	12	12	12	12	at.%			
Si	1.989	1.996	1.990	1.991	2.008	2.972	2.989	2.998	2.986	2.968	S	52.0	46.6	52.3
Ti	0.014	0.016	0.013	0.015	0.015	0.025	0.026	0.024	0.026	0.026	Fe	47.7	24.5	23.7
Al	0.402	0.330	0.429	0.329	0.342	1.942	1.936	1.936	1.93	1.93	Co	0	1.40	0
Cr	0.001	0.001	0.000	0.002	0.002	0.002	0.002	0.004	0.002	0.004	Ni	0.290	27.4	0
Mg	0.570	0.676	0.545	0.682	0.62	1.685	1.918	1.678	1.932	1.782	Cu	0.043	0	23.6
Ca	0.439	0.481	0.423	0.483	0.467	0.325	0.266	0.322	0.266	0.304	Si	0.009	0.017	0.366
Mn	0.003	0.002	0.003	0.003	0.002	0.021	0.019	0.020	0.018	0.020				
Fe	0.166	0.150	0.156	0.152	0.17	1.046	0.844	1.014	0.846	0.99				
Na	0.417	0.334	0.440	0.338	0.349	0.024	0.022	0.020	0.024	0.024				
K	0.006	0.006	0.006	0.006	0.006	0.000	0.000	0.000	0.000	0.000				
Totals	4.007	3.993	4.005	4.001	3.981	8.042	8.026	8.016	8.030	8.048				
Mg#	77	82	78	82	78	62	69	62	70	64				
En/Py	49	52	49	59	57	56	64	64	64	64				
Fs/Al	14	11	14	33	25	35	28	28	28	28				
Wo/Gr	37	37	37	4	4	9	8	8	8	8				

Clinopyroxene and garnet are from different locations in UD-111/02 (per Fig. 1). Abbreviations are: n.a.: not analyzed; Cpx, clinopyroxene; Gt, garnet; En, enstatite; Py, pyrope; Fs, ferrosilite; Al, almandine; Wo, wollastonite; Gr, grossular; Po, pyrrhotite; Pn, pentlandite; Cpy, chalcopyrite.
[a] Mineral pairs next to each other were used for calculating temperature.

Diamond faces are often stepped (striated), and many diamonds contain cracks, some radiating to the surface.

Cathodoluminescence (CL) of diamond is mainly caused by N defects in the crystal structure. Most diamonds in UD-111/02 have a typical blue cathodoluminescent color. A yellow-green cathodoluminescence was present in two diamonds (e.g., D-64). A similar CL color in diamonds from other kimberlites was suggested to be associated with lower nitrogen contents than blue-green CL colors (e.g., Kaapvaal, South Africa: Harte et al., 1999; Mir pipe: Bulanova et al., 2002; George Creek, Colorado: Fitzsimons et al., 1999).

The CL zonings of 24 diamonds, coupled with those of 12 diamonds from Stepanov et al. (2007), can be divided into two main types showing weak correlation with size and shape. The first type of diamond contains a bright CL interior with a dark non-luminescent (or dark-blue) rim (D-5b1, D-15, D-38, D-60b, D-64, D-73, Fig. 5). The bright interiors contain coarse, bright, octahedral-growth zones, interspersed with dark zones. The dark rims contain curved, weakly luminescent-growth zones, usually ascribed to fibrous diamond resulting from rapid growth, typically due to interaction with kimberlite melt (e.g., Anand et al., 2004). All >1 mm octahedral diamonds belong to this type. The interiors of four larger diamonds (3–5 mm) display cores with jagged boundaries (D-5b1, D-31, D-38, and D-73 in Fig. 5), truncated by later growth zones, demonstrating resorption features and multiple-growth episodes. Two diamonds (D-29 and D-31) have thinner dark rims. However, diamonds extracted in the vicinity of these two diamonds have thicker rims (compare D-29 and D-60b in Fig. 5). The second type of diamonds is generally ≤1 mm cubo-octahedral diamonds with only weak CL intensities, comparable to the rims of larger octahedral diamonds. The weak CL zoning in these diamonds is only visible after image manipulation (e.g., D-35 and D-81 in Fig. 5).

3.4. In-situ measurement of carbon isotopes of diamond

The total range of $\delta^{13}C$ of sixteen diamonds from our portion of UD-111/02 is −9.2 to −2.0‰ (Figs. 5 and 6, Table 2), which is slightly larger than that observed by Stepanov et al. (2007) on two diamonds (−3.7 to −6.2‰). There is no clear correlation between CL intensity and $\delta^{13}C$, consistent with the results of Harte et al. (1999) and Stepanov et al. (2007). Dark CL rims of all diamonds (26 analyses) have an average $\delta^{13}C$ value of −5.2‰ with a 2SD of 1.2‰, similar to the average mantle value of −5.5‰ by Kirkley et al. (1991). Intermediate zones of fifteen diamonds (51 analyses) are also similar to rims with an average value of −5.3‰ and a 2SD of 1.4‰. Most diamond cores/centers (−4.4 to −7.1‰) are similar within 2SD to the intermediate zones and rims. These values coincide the range of the octahedral and cubic microdiamonds from the Udachnaya pipe (Reutsky and Zedgenizov, 2007) and diamonds in other eclogites of the Udachnaya pipe (Snyder et al., 1995). However, three diamonds contain regions of significantly different $\delta^{13}C$ values from the average value (−5.2‰). A dark, irregular CL "core" in diamond D-31 contains $\delta^{13}C$ values of −9.2‰, whereas diamond D-73 shows a jagged core with $\delta^{13}C$ values of −3.3‰ (Fig. 5). Reproducibility of these 'abnormal' values is shown by multiple analyses in the vicinity (Fig. 5). The intermediate and rim zones of these two diamonds have similar $\delta^{13}C$ values (−4.2 to −5.3‰). A small non-luminescent, cubo-octahedral diamond (D-35) (Fig. 5) contains a core enriched in ^{13}C ($\delta^{13}C$ = −2.0‰), which is the highest value observed in UD-111/02 diamonds.

3.5. Compositions of inclusions

Many of the extracted diamonds from our portion of UD-111/02 contain sulfide and clinopyroxene inclusions. Stepanov et al. (2008) reported garnet inclusions in the other portion of UD-111/02. Inclusions, especially sulfides, are generally associated with cracks. Clinopyroxene inclusions are 10 to 100 μm in size. Some clinopyroxenes, examined after exposure on a polished diamond surface, have the same spongy texture as with most of the clinopyroxenes in the host eclogite (Fig. 7). Similar textures were observed by Taylor et al. (2000). The cubo-octahedral morphology of these spongy

Please cite this article as: Liu, Y., et al., Metasomatic origin of diamonds in the world's largest diamondiferous eclogite, Lithos (2009), doi:10.1016/j.lithos.2009.06.036

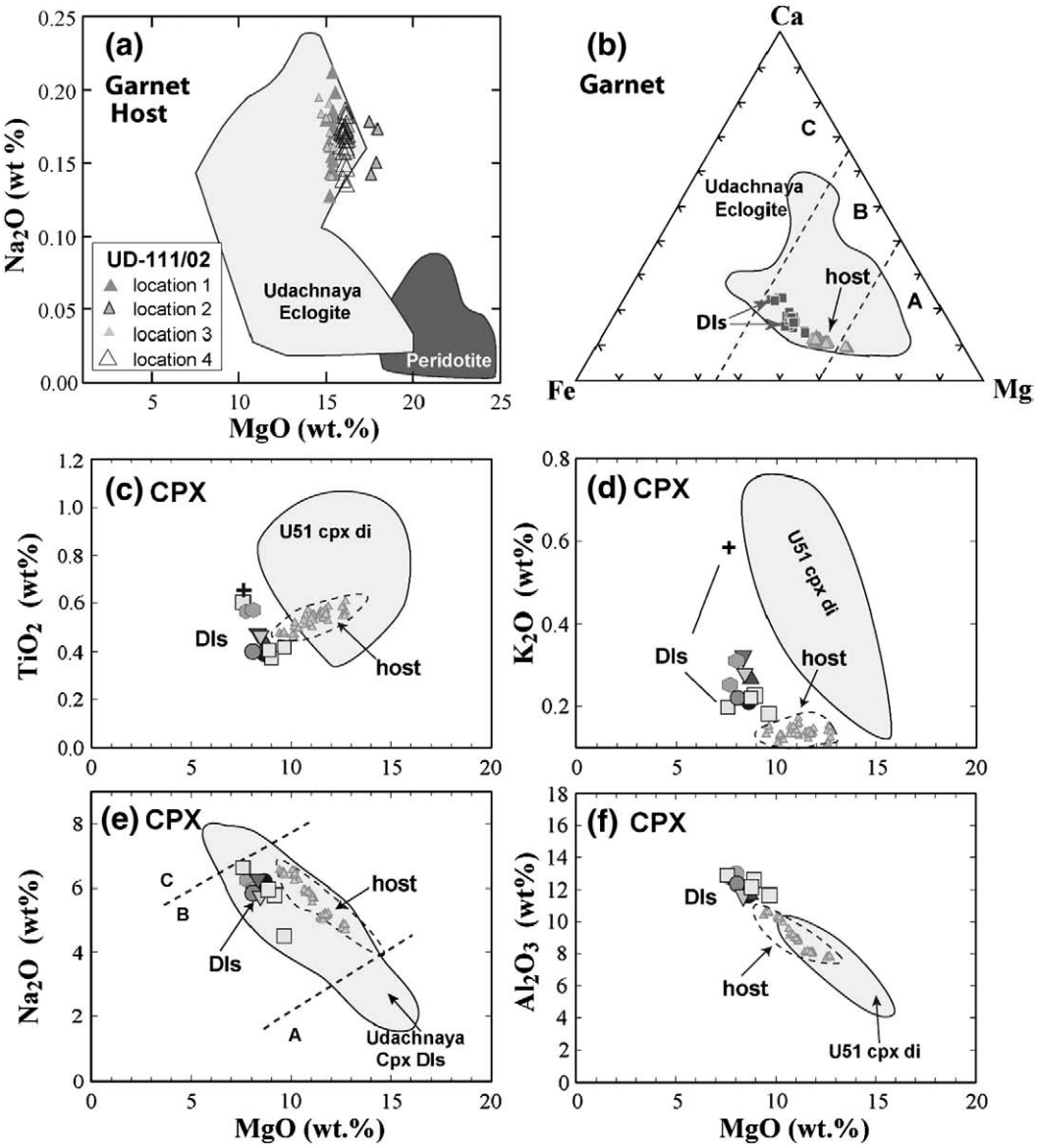

Fig. 4. Compositions of pristine silicate minerals as host (small gray triangles pointing up) and as diamond inclusions (DIs) in UD-111/02. (a) and (b) show compositions of pristine garnet host and DIs in UD-111/02. Garnet DIs are from Stepanov et al. (2008). A, B, C in (b) are three Groups of eclogites of Taylor and Neal (1989). Light gray fields outline garnet hosts in other eclogite xenoliths from Udachnaya kimberlite pipe (Taylor and Anand, 2004). (c)–(f) Compositions of pristine clinopyroxene host (small triangles pointing up) and DIs in UD-111/02. Same symbols are inclusions from the same diamond. Dashed curves encircle the host clinopyroxene range. The fields in (c), (d), and (f) plot clinopyroxene DIs from the Udachnaya diamondiferous eclogite U-51 (Taylor et al., 2000). The field in (e) plots clinopyroxene DIs from other Udachnaya eclogite xenoliths (Taylor and Anand, 2004).

clinopyroxenes has been proposed to indicate their syngenetic nature (Meyer, 1987), an interpretation questioned by Taylor et al. (2003).

The non-spongy-textured, 'pristine' clinopyroxene inclusions are all single-crystals of omphacite and belong to the Group B pyroxenes (Fig. 4e; Taylor and Neal, 1989). Individual pristine inclusions are totally homogeneous. Compared to the host clinopyroxene (Fig. 4c–f), pristine inclusions contain distinctly higher contents of K_2O and Al_2O_3, but slightly lower Na_2O and Mg# (72–75), similar to that reported by Taylor et al. (1996, 1998, 2000), and both corresponding to higher pressures of equilibration. All clinopyroxene inclusions from the UD-111/02 diamonds differ from each other measurably in chemistry (4.5–6.6 wt.% Na_2O; 7.5–9.6 wt.% MgO). Three inclusions from a single diamond (D-15) also have slightly different compositions, although they are all in the same growth zone (Table 3, Fig. 5), a finding never reported before. Garnet inclusions show a compositional range in major elements, slightly higher in CaO and FeO than the host garnet. Stepanov et al. (2008) reported the typical convex upward patterns for chondrite-normalized REEs in garnets from diamond inclusions. They also showed variations in trace elements in other silicate inclusions: LREE for clinopyroxene inclusions differed by a factor of ~20 for La and MREE for garnet inclusions (by a factor of ~5). Compared to host minerals, clinopyroxene inclusions are depleted in LREEs (La, Ce), and most garnet inclusions contain similar REEs.

4. Discussion

4.1. Diamond genesis in UD-111/02

Compositional variations of mineral inclusions in UD-111/02 are inconsistent with a single homogeneous growth event for diamonds. Inclusions from different diamonds (Fig. 4) show considerable variation in both major- and trace-element contents, suggesting

Please cite this article as: Liu, Y., et al., Metasomatic origin of diamonds in the world's largest diamondiferous eclogite, Lithos (2009), doi:10.1016/j.lithos.2009.06.036

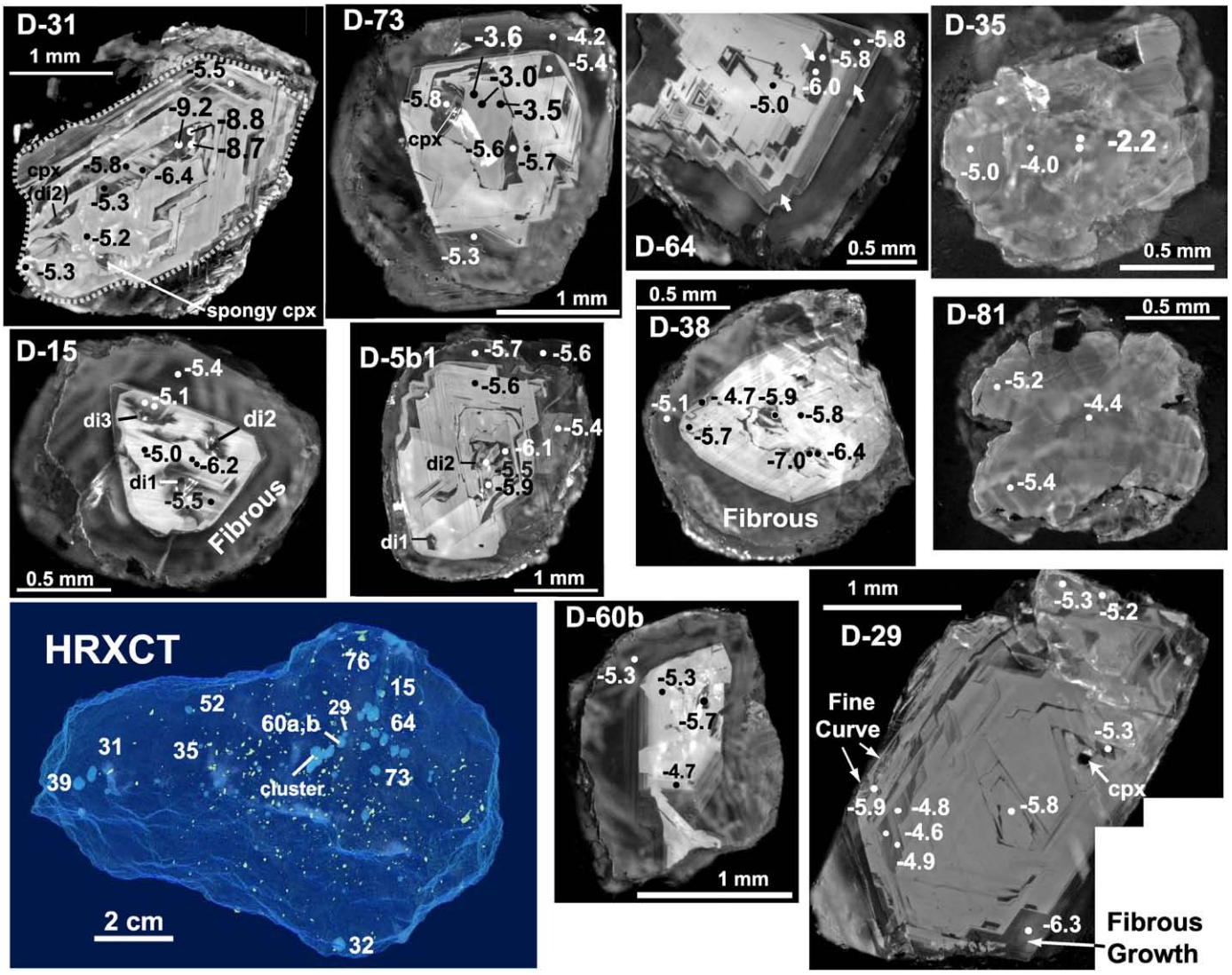

Fig. 5. Cathodoluminescence (CL) zonings of polished diamond plates. All CL images are on grayscale. The yellow-green color of a luminescent zone in D-64 was marked by arrows. Irregular cores inside the bright CL region can be discerned in D-5b1, D-31, D-38, and D-73. Dashed curve in D-31 marks the edge of polished plate. Note the finely curved CL zones at the edge of D-29. The carbon-isotope ratios ($\delta^{13}C$) and the ion-microprobe analytical spots are marked filled circles, size of which is larger than the true spot size for illustration purposes. Clinopyroxene inclusions are also labeled (Table 3). Locations of diamonds inside the UD-111/02 are shown in the 3-d HRXCT of the sample in the lower left.

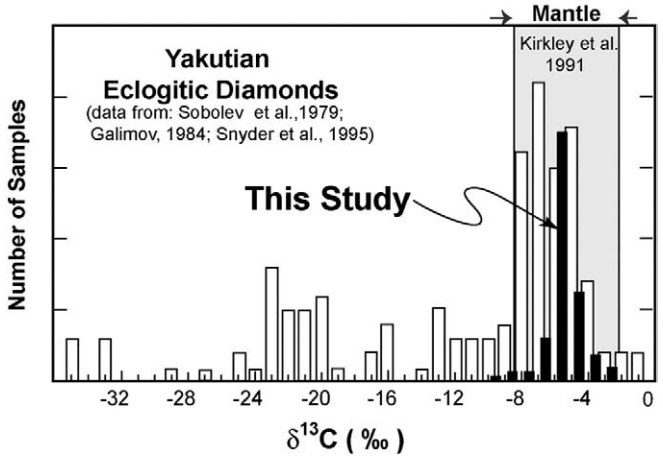

Fig. 6. Histogram of the $\delta^{13}C$ values of sixteen UD-111/02 diamonds (black bars) measured *in-situ* by ion microprobe, as compared with literature data (open bars; Sobolev et al., 1979; Galimov, 1984; Snyder et al., 1995) on Yakutian eclogitic diamonds.

they may have been encapsulated at different times in the ever-changing nature of the host (if protogenetic), or they are the result of many different metasomatic-fluid compositions. The higher K_2O in clinopyroxene included within diamond, compared to host minerals, suggests that they were encapsulated at higher pressures and/or the host rock has re-equilibrated to lower *P–T* (Harlow, 1997).

The 'stratigraphy', that is, the relationship of the nitrogen aggregation (CL) zones, does not appear to correlate between different diamonds from this single xenolith, let alone in several diamondiferous eclogites studied. This strongly supports our contention that diamonds in UD-111/02 were formed in multiple metasomatic stages. Diamond cores with jagged CL boundaries (e.g., D-31, D-73 in Fig. 5) represent resorption of early-formed diamonds by interaction with different metasomatic fluids. The dark CL rims and small diamonds with weak CL zones probably formed from kimberlite fluids at some stage during their transport by the kimberlite. The bright CL interiors of diamonds (Fig. 5) represent different fluids from those of the later kimberlite; CL intensity is a function of minor dislocations caused by the N aggregation state in diamond, which is a function of temperature, N abundances, and growth rate of diamond (Mendelssohn and Milledge, 1995). This proposed

Please cite this article as: Liu, Y., et al., Metasomatic origin of diamonds in the world's largest diamondiferous eclogite, Lithos (2009), doi:10.1016/j.lithos.2009.06.036

Table 2
Values of $\delta^{13}C$ in diamonds analyzed *in-situ* by SIMS[a] at the University of Wisconsin.

Crystal	Point location	$\delta^{13}C$	Error (2σ)		Point location	$\delta^{13}C$	Error (2σ)
D-5b1	Center	−5.9	0.4	D-64 oct.	Intermediate	−5.0	0.5
intergrown	Center	−5.5	0.4		Intermediate	−5.4	0.5
with 5b	Center	−6.1	0.4		Intermediate	−5.8	0.5
striated oct.	Intermediate	−5.6	0.4		Intermediate	−6.0	0.5
	Intermediate	−5.4	0.4		Intermediate	−5.8	0.5
	Rim	−5.7	0.4		Rim	−4.6	0.5
	Rim	−5.6	0.4				
				D-65	Center	−5.8	0.6
D-15	Intermediate	−6.2	0.3	3 intergrown	Center	−5.9	0.6
striated oct.	Intermediate	−5.1	0.4	oct.	Intermediate	−6.0	0.6
	Intermediate	−6.0	0.4		Intermediate	−4.8	0.6
	Intermediate	−5.2	0.4		Rim	−4.8	0.6
	Intermediate	−5.5	0.3				
	Intermediate	−5.1	0.3	D-73	Center	**−3.0**[b]	0.6
	Intermediate	−4.7	0.4	striated oct.	Center	**−3.6**	0.5
	Rim	−5.4	0.3		Center	**−3.5**	0.5
					Intermediate	−5.8	0.6
D-22	Intermediate	−5.7	0.4		Intermediate	−5.6	0.6
striated oct.	Intermediate	−5.6	0.4		Intermediate	−5.7	0.6
rounded	Intermediate	−5.0	0.4		Intermediate	−5.4	0.6
edge	Intermediate	−4.9	0.4		Intermediate	−5.3	0.6
	Intermediate	−4.2	0.4		Rim	−4.2	0.6
	Intermediate	−4.6	0.4				
	Rim	−4.8	0.4	D-76 oct.	Center	−5.9	0.4
				resorbed	Intermediate	−5.0	0.4
D-29 oct.	Center	−5.2	0.3	edge	Intermediate	−5.4	0.4
	Center	−5.8	0.3		Intermediate	−5.2	0.4
	Intermediate	−4.6	0.3		Intermediate	−6.5	0.4
	Intermediate	−4.8	0.3		Intermediate	−7.1	0.4
	Intermediate	−4.9	0.3		Intermediate	−6.2	0.4
	Rim	−5.9	0.3		Rim	−5.7	0.4
	Rim	−6.3	0.3		Rim	−4.7	0.4
	Rim	−5.3	0.3		Rim	−5.2	0.4
	Rim	−5.1	0.3				
				D-81	Center	−4.4	0.3
D-31 oct.	Center	**−9.2**	0.3	cubo-oct.	Rim	−5.2	0.3
	Center	**−8.8**	0.3		Rim	−5.4	0.3
	Center	**−8.7**	0.3				
	Center	−6.4	0.3	D-35	Center	**−2.4**	0.6
	Center	−5.8	0.3	cubo-oct.	Center	**−3.7**	0.5
	Intermediate	−5.2	0.3		Center	**−2.0**	0.5
	Intermediate	−5.3	0.3		Intermediate	−4.0	0.5
	Rim	−5.3	0.3		Rim	−5.0	0.6
	Rim	−5.5	0.3		Rim	−5.8	0.5
D-38	Center	−7.1	0.4	D-42	Center	−5.7	0.4
striated	Center	−6.4	0.4	oct. with	Intermediate	−5.5	0.4
oct.	Intermediate	−5.8	0.4	extended	Intermediate	−3.9	0.4
	Intermediate	−5.9	0.4	growth on	Intermediate	−4.7	0.4
	Intermediate	−5.9	0.4	(111)	Intermediate	−5.6	0.4
	Intermediate	−5.7	0.4		Rim	−5.1	0.4
	Intermediate	−4.7	0.4				
	Rim	−5.0	0.4				
D-52	Center	−4.8	0.6	D-60b	Intermediate	−5.7	0.3
striated	Intermediate	−3.2	0.6	intergrown	Intermediate	−5.2	0.3
oct.	Intermediate	−4.7	0.6	with 60a;	Intermediate	−4.7	0.3
	Rim	−3.6	0.6	brown	Rim	−5.3	0.3
				striated oct.			
D-54	Intermediate	−5.5	0.3				
cubo-oct.	Rim	−6.1	0.3				
	Rim	−5.8	0.3				

[a] All analyses were reported in ‰ $\delta^{13}C_{PDB}$, which is defined as $(^{13}C/^{12}C_{sample} - {}^{13}C/{}^{12}C_{PDB})/(^{13}C/^{12}C_{PDB}) * 1000$. Analytical error was estimated by bracketing sample analyses with 8 to 12 analyses on an in-house standard (see text).

[b] Bold numbers are values significantly different (outside the 2σ range of ±1.4‰) from the majority of values (average −5.3‰). The reproducibility of these values is shown by multiple analyses.

petrogenetic evolution of these diamonds is consistent with nitrogen contents and degrees of N aggregation; Stepanov et al. (2007) have also reported the CL zonations to indicate two stages of formation of these diamonds.

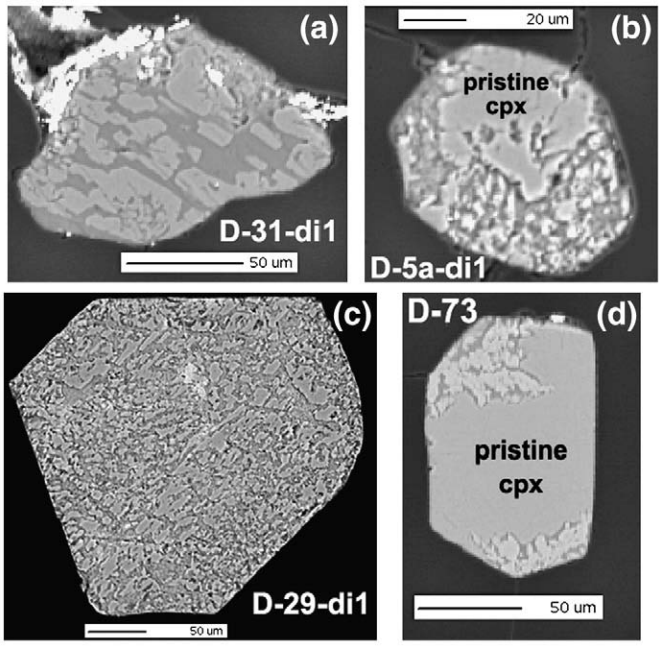

Fig. 7. Back-scattered electron (BSE) images of clinopyroxene inclusions exhibiting spongy textures of secondary alteration in UD-111/02 diamonds. a, b, and d are inclusions exposed on a polished surface. The bright materials in these images are Au left in cracks and depressions from the SIMS study. c is an inclusion extracted from diamond D-29. This inclusion was mounted in epoxy and polished for EMP study.

The carbon-isotope systematics in these diamonds are also consistent with multiple-growth events and with possible multiple sources for the carbon chemistry of the diamond. The different $\delta^{13}C$ values of CL-distinctive diamond cores are not comparable to formation from the same fluids as intermediate zones (bright CL) and rims. Experimental studies of carbon isotopes in synthetic diamonds (Reutsky et al., 2008a,b) reported that early-crystallized diamonds from Fe–Ni–C melts are enriched in $\delta^{13}C$ (by 3.3‰) due to non-steady-state fractionation in a closed system between diamonds and melts; late-formed diamonds will have the same $\delta^{13}C$ as initial source melts as a result of steady-state fractionation. These empirical experimental results would imply that the diamonds formed from non-steady-state fractionation from a mantle fluid ($\delta^{13}C = -5.5‰$) would have $\delta^{13}C$ of −2.0‰, similar to the center of the weak CL diamond (D-35, Fig. 5). However, this cannot explain diamond cores with $\delta^{13}C$ of −9.2‰ (D-31) nor the appearance of −9.2 and −3.3‰ cores in diamonds of similar size. Therefore, we suggest that these diamonds (D-31 and D-73 cores) crystallized from different fluids from each other and from later-formed intermediate zones and rims. Alternatively, the total range of $\delta^{13}C$ in UD-111/02 diamonds is consistent with those produced by Rayleigh fractionation between the diamond-forming fluids and CO_2 gas (Deines, 1980), possibly as a result of changing oxygen fugacity at constant T and P. Different core $\delta^{13}C$ values for diamond D-31 and D-73 would suggest a large change in oxygen fugacity on the decameter scale, or they formed from different fluids.

Combining evidences from the data observations and explanations above, we suggest that: 1) the isotopically and texturally distinct diamond cores may have formed from different fluids and followed by subsequent resorption due to a change of environment; 2) diamonds with bright CL formed in fluids at different temperatures or grew at different rates from those of the rims; and 3) the dark CL rims of large diamonds and small weakly-zoned diamonds formed by late-stage interaction of diamond with kimberlite fluids. The lineation of diamonds in alteration veins and presence of diamond clusters with resorption features in UD-111/02 suggest that alteration zones provide pathways for this process. Such complex

Please cite this article as: Liu, Y., et al., Metasomatic origin of diamonds in the world's largest diamondiferous eclogite, Lithos (2009), doi:10.1016/j.lithos.2009.06.036

Table 3
Composition of pristine clinopyroxene inclusions in diamonds from UD-111/02.

N[a]	D-5a 3	D-5b1-di1 6	D-5b1-di2 3	D-15-di1 3	D-15-di2 5	D-15-di3 3	D-31-di2 4	D-43 3	D-60 3	D-65 4	D-73 6	D-76 3
SiO_2	54.8 (2)	55.1 (3)	56.8 (9)	55.5 (5)	56.2 (3)	55.8 (4)	55.4 (3)	56.5 (3)	56.3 (2)	55.7 (6)	55.9 (3)	55.5 (1)
TiO_2	0.42 (4)	0.57 (1)	0.57 (3)	0.42 (4)	0.38 (2)	0.41 (2)	0.63 (4)	0.47 (1)	0.40 (0)	0.48 (1)	0.60 (4)	0.39 (1)
Al_2O_3	11.7 (1)	12.6 (1)	12.8 (4)	10.9 (1)	11.7 (1)	11.8 (1)	12.5 (1)	11.7 (1)	12.3 (1)	12.2 (3)	12.9 (0)	11.3 (1)
Cr_2O_3	0.07 (2)	0.08 (1)	0.08 (0)	0.04 (1)	0.06 (3)	0.05 (3)	0.07 (2)	0.05 (4)	0.06 (4)	0.03 (1)	0.06 (2)	0.08 (4)
MgO	8.74 (21)	7.75 (5)	8.06 (23)	9.63 (11)	8.88 (11)	8.73 (6)	7.64 (4)	8.44 (10)	8.11 (38)	8.33 (22)	7.59 (11)	8.68 (9)
CaO	11.2 (0)	11.1 (0)	11.3 (2)	12.0 (1)	11.1 (1)	11.1 (0)	11.1 (1)	11.0 (1)	10.9 (3)	11.1 (1)	11.2 (1)	11.0 (2)
MnO	0.07 (2)	0.05 (1)	0.05 (5)	0.08 (1)	0.06 (1)	0.06 (4)	0.06 (3)	0.09 (3)	0.08 (4)	0.07 (2)	0.05 (1)	0.07 (2)
FeO	5.56 (10)	4.75 (10)	4.97 (14)	5.87 (4)	5.50 (2)	5.57 (2)	4.79 (13)	5.92 (3)	5.22 (1)	5.23 (6)	4.83 (10)	5.61 (24)
Na_2O	5.94 (24)	6.24 (12)	5.96 (13)	4.51 (46)	5.81 (7)	5.96 (8)	6.51 (5)	5.76 (4)	5.82 (26)	6.27 (15)	6.61 (14)	6.19 (1)
K_2O	0.27 (1)	0.25 (2)	0.31 (1)	0.18 (2)	0.22 (2)	0.22 (2)	0.59 (3)	0.28 (1)	0.22 (1)	0.32 (2)	0.20 (2)	0.21 (1)
Totals	98.8	98.4	100.9	99.2	99.8	99.7	99.3	100.1	99.4	99.6	99.9	99.3
Oxygen	6	6	6	6	6	6	6	6	6	6	6	6
Si	1.974	1.978	1.987	1.987	1.992	1.985	1.978	1.999	2.000	1.982	1.980	1.989
Ti	0.011	0.015	0.015	0.012	0.010	0.011	0.017	0.012	0.011	0.013	0.016	0.010
Al	0.496	0.534	0.530	0.461	0.489	0.495	0.528	0.487	0.516	0.510	0.537	0.488
Cr	0.002	0.002	0.002	0.001	0.001	0.002	0.002	0.001	0.002	0.001	0.002	0.002
Mg	0.469	0.415	0.421	0.514	0.470	0.463	0.407	0.445	0.429	0.442	0.401	0.461
Ca	0.431	0.426	0.424	0.460	0.421	0.422	0.425	0.418	0.414	0.421	0.423	0.424
Mn	0.002	0.001	0.001	0.003	0.002	0.002	0.002	0.003	0.003	0.002	0.002	0.002
Fe	0.167	0.143	0.146	0.176	0.163	0.165	0.143	0.175	0.155	0.156	0.143	0.168
Na	0.415	0.435	0.404	0.313	0.399	0.411	0.451	0.395	0.401	0.433	0.454	0.414
K	0.012	0.012	0.014	0.008	0.010	0.010	0.027	0.013	0.010	0.015	0.009	0.010
	3.979	3.961	3.942	3.933	3.958	3.966	3.979	3.948	3.938	3.973	3.966	3.967
Mg#	74	74	74	75	74	74	74	72	73	74	74	73

[a] *N* is total number of analyses of individual inclusions. Numbers in brackets are one standard deviation of the last decimal, determined by multiple analyses of the individual inclusion.

diamond evolution did not occur synchronously with eclogite formation; rather, diamonds crystallized over a period of time, under variable conditions, from different metasomatic fluids, perhaps long after the subducted oceanic crust metamorphosed to eclogite (Taylor and Anand, 2004).

4.2. Evidence for multiple metasomatic events in other diamondiferous eclogites

Our conclusions drawn from the world's largest diamondiferous eclogite are in no way unique. Lineations of diamonds in alteration veins have been observed in other Udachnaya eclogites (Keller et al., 1999; Taylor et al., 2000; Spetsius and Taylor, 2002; Anand et al., 2004; Stepanov et al., 2007, 2008; L.A. Taylor, unpublished data) and diamondiferous eclogite from Roberts Victor kimberlite, South Africa (Schulze et al., 1996; Ishikawa et al., 2008). Multi-stage formation of diamonds was proposed based on a wide range multiple-inclusion compositions (both major- and trace-element) from single diamonds and inclusions from several diamonds from single xenoliths from Yakutian kimberlites (e.g., Jerde et al., 1993; Taylor et al., 1996, 1998, 2000, 2003; Shatsky et al., 2008).

Complex CL zones have been reported for individual diamonds and multiple diamonds from a single xenolith (e.g., Bulanova, 1995; Taylor et al., 2000; Bulanova et al., 2002; Anand et al., 2004; Spetsius et al., 2008). The complex CL zones of individual diamonds with multiple-growth and resorption features are regarded as *incomparable* with single-stage growth of diamonds simultaneously with the host eclogite. Taylor et al. (2000) reported a diamond with intense plastic deformation features from a Udachnaya diamondiferous eclogite (U51), indicating an extremely complicated and torturous growth history for that particular diamond. Coexistence of diamonds with and without plastic deformation in the same rock poses additional challenges for the synchronous formation of all diamonds within the host rock. Taylor et al. (2000) proposed that the diversity in both mineral inclusions and CL features could be a result of diamonds moving inside the relatively softer host eclogite in the asthenosphere, seeing different growth environments, and at the same time being affected by various metasomatic fluids. This is in general agreement with large compositional variation of host minerals on a small scale (i.e., cm) in Yakutian eclogites (Beard et al., 1996), and with those layered eclogites from Roberts Victor kimberlites (Jacob and Jagoutz, 1994; Ishikawa et al., 2008).

Globally, eclogitic diamonds display a wide range in carbon isotopes from +5 to −41‰ (Kirkley et al., 1991; Cartigny, 2005; De Stefano et al., 2008), whereas diamonds from single kimberlite pipes show significant, but smaller, ranges of variation in $\delta^{13}C$ (e.g. Deines, 1980). Carbon-isotope data for multiple diamonds from a single xenolith are rare (Taylor and Milledge, 1995; Stepanov et al., 2007; Ishikawa et al., 2008; Palot et al., 2008). Taylor and Milledge (1995), Ishikawa et al. (2008) and Palot et al. (2008) reported a limited range of variation in $\delta^{13}C$ (−4 to −7‰) in diamonds from individual xenoliths from different South Africa kimberlite pipes. However, all three studies analyzed chips of diamonds representing an averaging of relatively large volumes and without spatial context. In other studies, carbon-isotope variations in individual diamonds from multiple xenoliths from a single kimberlite pipe were determined in order to constrain the processes affecting the growth of diamonds (Swart et al., 1983; Javoy et al., 1984; Boyd et al., 1987; Harte and Otter, 1992; Fitzsimons et al., 1999; Harte et al., 1999; Taylor et al., 2000; Bulanova et al., 2002; Hauri et al., 2002; Zedgenizov and Harte, 2004; Zedgenizov et al., 2006; Thomassot et al., 2007). The complex patterns of carbon and nitrogen isotopes from core to rim of individual diamonds (e.g., Bulanova et al., 2002; Hauri et al., 2002; Zedgenizov and Harte, 2004; Zedgenizov et al., 2006) commonly show a range too large for isotope fractionation or growth-controlled fractionation.

5. Summary

The “pull-apart” dissection of the world's largest diamondiferous eclogite has revealed several significant features. These observations include: a) lineation of diamonds in alteration zones; b) clusters of dodecahedral diamonds (resorption morphology); c) diamonds in the same xenolith with different growth zones from core to rim; d) diamonds of decidedly different carbon-isotope values in/near the

Please cite this article as: Liu, Y., et al., Metasomatic origin of diamonds in the world's largest diamondiferous eclogite, Lithos (2009), doi:10.1016/j.lithos.2009.06.036

cores (both high and low $\delta^{13}C$) from rims; e) different chemistries between diamond inclusions and host minerals; and f) heterogeneity of mineral compositions in the host. Collectively, they support and re-enforce the conclusion that formation of diamonds in this eclogite was a multi-stage process involving several metasomatic-fluid events. The supporting observations above are by no means unique to this eclogite, as they have been previously documented and published on other diamondiferous eclogites (e.g., Taylor et al., 1996; Sobolev et al., 1998b; Taylor et al., 2000; Spetsius and Taylor, 2002; Anand et al., 2004; Shatsky et al., 2008). Thus, we conclude that the formation of diamonds in most mantle eclogites involves repeated resorption and growth companied by plastic deformation, indicating a torturous life of complicated growth to mantle diamonds, perhaps more normal a diamond life style than previously understood.

Acknowledgements

The research reported in this paper would not have been possible without the cooperation and collaboration of our several colleagues in the V.S. Sobolev Institute of Geology and Mineralogy of the Siberian Branch of the Russian Academy of Sciences in Novosibirsk. Allan Patchen is recognized for his assistance with the EMP analyses. We thank two anonymous reviewers for their constructive comments. A portion of the research was supported by the Planetary Geosciences Institute of the Department of Earth and Planetary Sciences at the University of Tennessee. Wisc-SIMS is partly supported by NSF (EAR03-19230, EAR07-44079) and the NASA Astrobiology Institute.

References

Anand, M., Taylor, L.A., Misra, K.C., Carlson, W.D., Sobolev, N.V., 2004. Nature of diamonds in Yakutian eclogites: views from eclogite tomography and mineral inclusions in diamonds. Lithos 77, 333–348.

Beard, B.L., Fraracci, K.N., Taylor, L.A., Snyder, G.A., Sobolev, N.V., 1996. Petrography and geochemistry of eclogites form the Mir kimberlite, Yakutia, Russia. Contributions to Mineralogy and Petrology 125, 293–310.

Boyd, S.R., Mattey, D.P., Pillinger, C.T., Milledge, H.J., Mendelssohn, M., Seal, M., 1987. Multiple growth events during diamond genesis — an integrated study of carbon and nitrogen isotopes and nitrogen aggregation state in coated stones. Earth and Planetary Science Letters 86, 341–353.

Boyd, F.R., Pokhilenko, N.P., Pearson, D.G., Mertzman, S.A., Sobolev, N.V., Finger, L.W., 1997. Composition of the Siberian cratonic mantle: evidence from Udachnaya peridotite xenoliths. Contributions to Mineralogy and Petrology 128, 228–246.

Bulanova, G.P., 1995. The formation of diamond. Journal of Geochemical Exploration 53, 1–23.

Bulanova, G.P., Pearson, D.G., Hauri, E.H., Griffin, B.J., 2002. Carbon and nitrogen isotope systematics within a sector-growth diamond from the Mir kimberlite, Yakutia. Chemical Geology 188, 105–123.

Carlson, W.D., Denison, C., 1992. Mechanisms of porphyroblast crystallization: results from high-resolution computed X-ray tomography. Science 257, 1236–1239.

Cartigny, P., 2005. Stable isotopes and the origin of diamond. Elements 1, 79–84.

Chaussidon, M., Albarede, F., Sheppard, S.M.F., 1987. Sulfur isotope heterogeneity in the mantle from ion microprobe measurements of sulfide inclusions in diamonds. Nature 330, 242–244.

De Stefano, A., Kopylova, M.G., Cartigny, P., Afanasiev, V., 2008. Diamonds and diamondiferous eclogites of the Jericho kimberlite (Northern Canada). 9th International Kimberlite Conference Extended Abstracts, No. 9IKC-A-00321.

Deines, P., 1980. The carbon isotopic composition of diamonds — relationship to diamond shape, color, occurrence and vapor composition. Geochimica et Cosmochimica Acta 44, 943–961.

Deines, P., Harris, J.W., 1995. Sulfide inclusion chemistry and carbon isotopes of African diamonds. Geochimica et Cosmochimica Acta 59, 3173–3188.

Durazzo, A., Taylor, L.A., 1982. Exsolution in the Mss-pentlandite system: textural and genetic implications for Ni-sulfide ores. Mineral Deposits 17, 313–332.

Eldridge, C.S., Compston, W., Williams, I.S., Harris, J.W., Bristow, J.W., 1991. Isotope evidence for the involvement of recycled sediments in diamond formation. Nature 353, 649–653.

Ellis, D.J., Green, D.H., 1979. An experimental study of the effect of Ca upon garnet–clinopyroxene Fe–Mg exchange equilibria. Contributions to Mineralogy and Petrology 71, 12–22.

Etschmann, B., Pring, A., Putnis, A., Grguric, B.A., Studer, A., 2004. A kinetic study of the exsolution of pentlandite $(Ni,Fe)_9S_8$ from the monosulfide solid solution (Fe,Ni)S. American Mineralogist 89, 39–50.

Fitzsimons, I.C.W., Harte, B., Chinn, I.L., Gurney, J.J., Taylor, W.R., 1999. Extreme chemical variation in complex diamonds from George Creek, Colorado: a SIMS study of carbon isotope composition and nitrogen abundance. Mineralogical Magazine 63, 857–878.

Galimov, E.M., 1984. The relation between formation conditions and variations in isotope composition of diamond. Geochemistry International 22, 118–141.

Griffin, W.L., Kaminsky, F.V., Ryan, C.G., O'Reilly, S.Y., Win, T.T., Ilupin, I.P., 1996. Thermal state and composition of the lithospheric mantle beneath the Daldyn kimberlite field, Yakutia. Tectonophysics 262, 19–33.

Harlow, G.E., 1997. K in clinopyroxene at high pressure and temperature: an experimental study. American Mineralogist 82, 259–269.

Harte, B., Otter, M.L., 1992. Carbon isotope measurements on diamonds. Chemical Geology 101, 177–183.

Harte, B., Fitzsimons, I.C.W., Harris, J.W., Otter, M.L., 1999. Carbon isotope ratios and nitrogen abundances in relation to cathodoluminescence characteristics for some diamonds from the Kaapvaal Province, S-Africa. Mineralogical Magazine 63, 829–856.

Hauri, E.H., Wang, J., Pearson, D.G., Bulanova, G.P., 2002. Microanalysis of $\delta^{13}C$, $\delta^{15}N$, and N abundances in diamonds by secondary ion mass spectrometry. Chemical Geology 185, 149–163.

Ishikawa, A., Pearson, D.G., Maruyama, S., Cartigny, P., Ketcham, R.A., Gurney, J.J., 2008. Compositional layering in a highly diamondiferous eclogite xenolith from the Roberts Victor kimberlite, South Africa and its implications for diamond genesis. 9th IKC, Abstract 00078.

Jacob, D.E., 2004. Nature and origin of eclogite xenoliths from kimberlites. Lithos 77, 295–316.

Jacob, D., Jagoutz, E., 1994. A diamond-graphite bearing eclogitic xenolith from Roberts Victor (South Africa): indications from petrogenesis from Pb-, Nd- and Sr-isotopes. In: Meyer, H.O.A., Leonardos, O.H. (Eds.), Kimberlites, Related Rocks and Mantle Xenoliths. Special Publication, vol. 1/A. CPRM, pp. 304–317.

Jacob, D.E., et al., 2009, this issue. Eclogite xenoliths from Kimberley, South Africa — A case study of mantle metasomatism in eclogites. Proceedings of the 9th International Kimberlite Conference. Lithos 112S, 1002–1013.

Javoy, M., Pineau, F., Demaiffe, D., 1984. Nitrogen and carbon isotopic composition in the diamonds of Mbuji Mayi (Zaire). Earth and Planetary Science Letters 68, 399–412.

Jerde, E.A., Taylor, L.A., Crozaz, G., Sobolev, N.V., Sobolev, V.N., 1993. Diamondiferous eclogites from Yakutia, Siberia — evidence for a diversity of protoliths. Contributions to Mineralogy and Petrology 114, 189–202.

Keller, R.A., Taylor, L.A., Snyder, G.A., Sobolev, V.N., Carlson, W.D., Bezborodov, S.M., Sobolev, N.V., 1999. Detailed Pullapart of a Diamondiferous Eclogite Xenolith: Implications for Mantle Processes during Diamond Genesis. In: Proceedings of the VIIth International Kimberlite Conference, vol. 1. Red Roof Design, Cape Town, pp. 397–402.

Kelly, D.P., Vaughan, D.J., 1983. Pyrrhotine–pentlandite ore textures — a mechanistic approach. Mineralogical Magazine 47, 453–463.

Kirkley, M.B., Gurney, J.J., Otter, M.L., Hill, S.J., Daniels, L.R., 1991. The application of C isotope measurements to the identification of the sources of C in diamonds — a review. Applied Geochemistry 6, 477–494.

Kita, N.T., Ushikubo, Takayuki, Fu, Bin and Valley, John W. 2009. High Precision SIMS Oxygen Isotope Analyses and the Effect of Sample Topography, Chemical Geology 264, 43–57.

Lowry, D., Mattey, D.P., Harris, J.W., 1999. Oxygen isotope composition of syngenetic inclusions in diamond from the Finsch Mine, RSA. Geochimica et Cosmochimica Acta 63, 1825–1836.

McCallum, M.E., Huntley, P.M., Falk, R.W., Otter, M.L., 1994. Morphological, resorption and etch feature trends of diamonds from kimberlite populations within Colorado–Wyoming State Line District, USA. In: Meyer, H.O.A., Leonardos, O.H. (Eds.), Diamonds: Characterisation, Genesis and Exploration. Special Publication, vol. 1/B. CPRM, pp. 32–50.

Mendelssohn, M.J., Milledge, H.J., 1995. Geologically significant information from routine analysis of the mid-infrared spectra of diamonds. International Geology Review 37, 95–110.

Meyer, H.O.A., 1987. Inclusions in diamond. In: Nixon, P.H. (Ed.), Mantle Xenoliths. John Wiley & Sons Ltd., Chichester, pp. 501–522.

Misra, K.C., Anand, M., Taylor, L.A., Sobolev, N.V., 2004. Multi-stage metasomatism of diamondiferous eclogite xenoliths from the Udachnaya kimberlite pipe, Yakutia, Siberia. Contributions to Mineralogy and Petrology 146, 696–714.

Palot, M., Cartigny, P., Viljoen, K.S., 2008. Diamond origin and genesis: a C and N stable isotope study on diamonds from a single eclogitic xenolith (Kaalvallei, South Africa). 9th IKC, Abstract 00184.

Pearson, D.G., Canil, D., Shirey, S.B., 2003. Mantle samples included in volcanic rocks: xenoliths and diamonds. Treatise on Geochemistry 2, 171–275.

Reutsky, V.N., Zedgenizov, D.A., 2007. Some specific features of genesis of micro-diamonds of octahedral and cubic habit from kimberlites of the Udachnaya pipe (Yakutia) inferred from carbon isotopes and main impurity defects. Russian Geology and Geophysics 48, 299–304.

Reutsky, V.N., Borzdov, Y.M., Palyanov, Y.N., 2008a. Carbon isotope fractionation associated with HPHT crystallization of diamond. Diamond and Related Materials 17, 1986–1989.

Reutsky, V.N., Harte, B., EIMF, Borzdov, Y.M., Palyanov, Y.N., 2008b. Monitoring diamond crystal growth, a combined experimental and SIMS study. European Journal Mineralogy 20, 365–374.

Robinson, D.N., 1979. Diamond and Graphite in Eclogite Xenoliths from Kimberlite: Proceedings of Second International Kimberlite Conference, vol. 2, pp. 50–58.

Rowe, T., Kappelman, J., Carlson, W.D., Ketcham, R.A., Denison, C., 1997. High-resolution computed tomography: a breakthrough technology for earth scientists. Geotimes 42, 23–27.

Ruzicka, A.M., Riciputi, L.R., Taylor, L.A., Snyder, G.A., Greenwood, J.P., Keller, R.A., Belanova, G.P., Milledge, H.J., 1999. Petrogenesis of mantle-derived sulfide inclusions in Yakutian diamonds; chemical and isotopic disequilibrium during

Please cite this article as: Liu, Y., et al., Metasomatic origin of diamonds in the world's largest diamondiferous eclogite, Lithos (2009), doi:10.1016/j.lithos.2009.06.036

quenching from high temperatures. Proceedings of the VIIth International Kimberlite Conference, vol. 2. Red Roof Design, Cape Town, pp. 741–749.
Schulze, D.J., Wiese, D., Steude, J., 1996. Abundance and distribution of diamonds in eclogite revealed by volume visualization of CT X-ray scans. Journal of Geology 104, 109–114.
Schulze, D.J., Harte, B., Valley, J.W., Brenan, J.M., Channer, D.M.D., 2003. Extreme crustal oxygen isotope signatures preserved in coesite in diamond. Nature 423, 68–70.
Shatsky, V., Ragozin, A., Zedgenizov, D., Mityukhin, S., 2008. Evidence for multistage evolution in a xenolith of diamond-bearing eclogite from Udachnaya kimberlite pipe. Lithos 105, 289–300.
Snyder, G.A., Taylor, L.A., Jerde, E.A., Clayton, R.N., Mayeda, T.K., Deines, P., Rossman, G.R., Sobolev, N.V., 1995. Archean mantle heterogeneity and the origin of diamondiferous eclogites, Siberia — evidence from stable isotopes and hydroxyl in garnet. American Mineralogist 80, 799–809.
Snyder, G.A., Taylor, L.A., Crozaz, G., Halliday, A.N., Beard, B.L., Sobolev, V.N., Sobolev, N.V., 1997. The origins of Yakutian eclogite xenoliths. Journal of Petrology 38, 85–113.
Sobolev, N.V., Galimov, E.M., Ivanovskaya, I.N., Yefimova, E.S., 1979. The carbon isotope compositions of diamonds containing crystalline inclusions. USSR Academy of Sciences, Doklady Earth Science Sections 249, 1217–1220.
Sobolev, V.N., Taylor, L.A., Snyder, G.A., Sobolev, N.V., 1994. Diamondiferous eclogites from the Udachnaya kimberlite pipe, Yakutia, Siberia. International Geology Review 36, 42–64.
Sobolev, N.V., Taylor, L.A., Zuev, V.M., Bezborodov, S.M., Snyder, G.A., Sobolev, V.N., Yefimova, E.S., 1998a. The specific features of eclogitic paragenesis of diamonds from Mir and Udachnaya kimberlite pipes (Yakutia). Geologiya i Geofizika 39, 1667–1678 (in Russian). English Translation: Russian Geology and Geophysics 39, 1653–1663.
Sobolev, N.V., Snyder, G.A., Taylor, L.A., Keller, R.A., Yefimova, E.S., Sobolev, V.N., Shimizu, N., 1998b. Extreme chemical diversity in the mantle during eclogitic diamond formation: evidence from 35 garnet and 5 pyroxene inclusions in a single diamond. International Geology Review 40, 567–578.
Sobolev, V.N., Taylor, L.A., Snyder, G.A., Jerde, E.A., Neal, C.R., Sobolev, N.V., 1999. Quantifying the effects of metasomatism in mantle xenoliths: constraints from secondary chemistry and mineralogy in Udachnaya Eclogites, Yakutia. International Geology Review 41, 391–416.
Spetsius, Z.V., Taylor, L.A., 2002. Partial melting in mantle eclogite xenoliths: connections with diamond paragenesis. International Geology Review 44, 973–987.
Spetsius, Z.V., Taylor, L.A., Valley, J.W., Deangelis, M.T., Spicuzza, M., Ivanov, A.S., Banzeruk, V.I., 2008. Diamondiferous xenoliths from crustal subduction: garnet oxygen isotopes from the Nyurbinskaya pipe, Yakutia. European Journal of Mineralogy 20, 375–385.
Spetsius, Z.V., et al., 2009, this issue. Combined C isotope and geochemical evidence for a recycled origin for diamondiferous eclogite xenoliths from kimberlites of Yakutia. Proceedings of the 9th International Kimberlite Conference. Lithos 112S, 1032–1042.
Stachel, T., Harris, J.W., 2008. The origin of cratonic diamonds — constraints from mineral inclusions. Ore Geology Reviews 34, 5–32.
Stepanov, A.S., Shatsky, V.S., Zedgenizov, D.A., Sobolev, N.V., 2007. Causes of variations in morphology and impurities of diamonds from the Udachnaya Pipe eclogite. Russian Geology and Geophysics 48, 758–769.
Stepanov, A.S., Shatsky, V.S., Zedgenizov, D.A., Sobolev, N.V., 2008. Chemical heterogeneity in the diamondiferous eclogite xenolith from the Udachnaya kimberlite pipe. Doklady Earth Sciences 419, 308–311.
Swart, P.K., Pillinger, C.T., Milledge, H.J., Seal, M., 1983. Carbon isotopic variation within individual diamonds. Nature 303, 793–795.
Taylor, L.A., Anand, M., 2004. Diamonds: time capsules from the Siberian Mantle. Chemie Der Erde-Geochemistry 64, 1–74.
Taylor, L.A., Liu, Y., 2009. Diamond sulfide inclusions are not Mss: exsolution of pyrrhotite, pentlandite, and chalcopyrite. V.S. Sobolev 100th Birthday Conference, 526 Proceedings (in revision).
Taylor, W.R., Milledge, H.J., 1995. Nitrogen aggregation character, thermal history, and stable isotope composition of some xenolith-derived diamonds from Roberts Victor and Finsch. Extended Abstracts of the 6th International Kimberlite Conference, Novosibirsk, pp. 620–622.
Taylor, L.A., Neal, C.R., 1989. Eclogites with oceanic crustal and mantle signatures from the Bellsbank kimberlite, South-Africa. 1. Mineralogy, petrography, and whole rock chemistry. Journal of Geology 97, 551–567.
Taylor, L.A., Snyder, G.A., Crozaz, G., Sobolev, V.N., Yefimova, E.S., Sobolev, N.V., 1996. Eclogitic inclusions in diamonds: evidence of complex mantle processes over time. Earth and Planetary Science Letters 142, 535–551.
Taylor, L.A., Milledge, H.J., Bulanova, G.P., Snyder, G.A., Keller, R.A., 1998. Metasomatic eclogitic diamond growth: evidence from multiple diamond inclusions. International Geology Review 40, 663–676.
Taylor, L.A., Keller, R.A., Snyder, G.A., Wang, W., Carlson, W.D., Hauri, E.H., McCandless, T., Kim, K.-R., Sobolev, N.V., Bezborodov, S.M., 2000. Diamonds and their mineral inclusions and what they tell us: a detailed "pull-apart" of a diamondiferous eclogite. International Geology Review 42, 959–983.
Taylor, L.A., Anand, M., Promprated, P., Floss, C., Sobolev, N.V., 2003. The significance of mineral inclusions in large diamonds from Yakutia, Russia. American Mineralogist 88 (5–6), 912–920.
Taylor, L.A., Ketchum, R., Day, J.M.D., Stepanov, A., Carlson, W., Shatsky, V., Sobolev, N.V., 2005. Gigantic diamondiferous eclogite from Udachnaya: mineralogy and tomography of this Yakutian xenolith. Eos Transactions AGU 86 (52) Fall Meet. Suppl., Abstract V43E-01.
Thomassot, E., Cartigny, P., Harris, J.W., Viljoen, K.S.F., 2007. Methane-related diamond crystallization in the Earth's mantle: stable isotope evidences from a single diamond-bearing xenolith. Earth and Planetary Science Letters 257, 362–371.
Zedgenizov, D.A., Harte, B., 2004. Microscale variations of $\delta^{13}C$ and N content within a natural diamond with mixed-habit growth. Chemical Geology 205, 169–175.
Zedgenizov, D.A., Harte, B., Shatsky, V.S., Politov, A.A., Rylov, G.M., Sobolev, N.V., 2006. Directional chemical variations in diamonds showing octahedral following cuboid growth. Contributions to Mineralogy and Petrology 151, 45–57.

Please cite this article as: Liu, Y., et al., Metasomatic origin of diamonds in the world's largest diamondiferous eclogite, Lithos (2009), doi:10.1016/j.lithos.2009.06.036